Full Paper

Synthesis and Biological Evaluation of Novel Farnesylthiosalicylic Acid Derivatives for Cancer Treatment

Yong Ling[1,2], Xuemin Wang[1], Hongyan Zhu[1], Zhiqiang Wang[1,2], Chenjun Xu[1], Xinyang Wang[1], Li Chen[2], and Wei Zhang[1]

[1] School of Pharmacy, Nantong University, Nantong, P. R. China
[2] State Key Laboratory of Natural Medicines, China Pharmaceutical University, Nanjing, P. R. China

Novel farnesylthiosalicylic acid (FTS) derivatives were synthesized by coupling with different substituted diamines. Their *in vitro* growth inhibitory activities against seven human cancer cell lines were evaluated. The results revealed that the synthetic farnesylthiosalicylamides displayed significant antitumor activities compared to the positive control FTS. Especially, compound **8f** exhibited the strongest antitumor activities with IC_{50} values of 6.20–7.83 μM, which were one- to threefold less than those of sorafenib and six- to tenfold less than that of FTS against each cell line *in vitro*. Furthermore, **8f** could inhibit the Ras-related signaling pathway and induce SMMC-7721 cell apoptosis superior to FTS in a dose-dependent manner. These data indicate that **8f** may hold greater promise as therapeutic agent for the intervention of human cancers.

Keywords: Antitumor activity / Diamines / Farnesylthiosalicylic acid / Ras-related signal pathway / Synthesis

Received: August 26, 2013; Revised: November 22, 2013; Accepted: November 22, 2013

DOI 10.1002/ardp.201300325

Introduction

Mutation and activation of Ras proto-oncogene and Ras signal pathway play a key role in regulating cell proliferation, migration, differentiation, and apoptosis [1–4]. The Ras proteins are membrane-anchored guanine-nucleotide binding proteins and function as biological switches that would act as a modulator of signal transduction pathways including mitogen-activated protein kinase (MAPK) and Akt [5, 6]. The disruption of GTPase activity due to oncogenic mutations leads to persistent Ras signaling and the excessive activation of Ras proteins that prompt the formation and progression of human malignant tumors [7, 8]. Additionally, the inhibition of excessive activated Ras proteins or Ras signal pathway has been shown to revert malignant cells to a nonmalignant phenotype and cause tumor regression both *in vitro* and *in vivo* [9]. Thus, the Ras proteins and its related signal pathway are attractive therapeutic targets for various cancers.

Farnesylthiosalicylic acid (FTS), acting as a Ras inhibitor which is an *S*-farnesyl cysteine analog, can recognize the anchorage and dislodge the active Ras protein from the cell membrane, thereby blocking the initiation of downstream signaling events, inhibiting tumor cell proliferation and promoting the tumor cell apoptosis [10–13]. FTS has been used for preclinical study of a wide range of malignancies, including liver, lung, breast, and pancreas cancers [13–16]. However, its therapeutic efficacy is limited [17]. Therefore, development of new Ras inhibitors with potent anti-tumor activity should be of particular clinical significance.

Diamines were excellent structural elements in medicinal chemistry possessing functions such as improving water-solubility of active molecules, contributing to potentiation of bioavailability, metabolic stability of molecules [18]. Moreover, various lead compounds and clinical candidates have contained the subunits of diamines [19]. In addition, Goldberg et al. [20] have reported that FTS-amide exhibited higher efficacy in inhibition of Ras-GTP and cell growth compared to FTS, and our previously studies have developed many promising farnesylthiosalicylamide derivatives which exhibited much stronger anti-hepatocellular carcinoma activities superior to FTS and the corresponding esters [21]. Accordingly, different substituted diamines were introduced to FTS with the purpose for further enhancement of anticancer activity. Therefore, a total of eight farnesylthiosalicylamide derivatives (**10a–h**) were designed and synthesized via the conjugation of

Correspondence: Prof. Wei Zhang, School of Pharmacy, Nantong University, Nantong 226001, P. R. China.
E-mail: zwei@ntu.edu.cn
Fax: +86 513 85051892

the carboxyl group of FTS with different substituted diamines. Their anticancer activities, Ras-related signal route, and apoptotic effects were evaluated *in vitro*. Herein, we report the synthesis and biological evaluation of these compounds.

Results and discussion

Chemistry

In this paper FTS was obtained from the starting material (*E*,*E*)-farnesol, and the synthesized FTS was regarded as parent compound and positive control in the study of antitumor activity for the ongoing investigation. The synthetic routes of **8a–h** were outlined in Scheme 1. (*E*,*E*)-Farnesol (**2**) was firstly treated with PBr_3 to form (*E*,*E*)-farnesyl bromide (**3**). In addition, carboxyl group of thiosalicylic acid (**4**) was protected by methyl esterification with methanol in the presence of $SOCl_2$ to obtain methyl thiosalicylate (**5**), which was then reacted with (*E*,*E*)-farnesyl bromide (**3**) under the condition of K_2CO_3 to obtain methyl (*E*,*E*)-farnesylthiosalicylicate (**8**). Then the parent compound FTS (**1**) was gained through the hydrolyzation of **8** with aqueous solution of NaOH. Finally, FTS was treated with oxalylchloride to give (*E*,*E*)-farnesylthiosalicyl chloride, and then different substituted diamines were reacted with (*E*,*E*)-farnesylthiosalicyl chloride in the presence of triethylamine to obtain target compounds **8a–h**. The products **8a–h** were purified by column chromatography, and their structures were characterized by IR, ^1H NMR, MS, and elemental analyses.

Biological evaluation

The inhibitory activities of synthetic compounds **8a–h** against seven human cancer cell lines SMMC-7721 (human hepatocellular carcinoma cells), Panc-1 (human pancreatic carcinoma cells), EJ (human bladder carcinoma cells), SGC7901 (human gastric cancer cells), SKOV-3 (human ovarian cancer cells), H460 (human lung cancer cells), and MCF-7 (human breast cancer cells) were evaluated by MTT assays *in vitro* with FTS and sorafenib as positive controls. The IC_{50} values of **8a–h** against the seven human cancer cell lines are listed in Table 1. The results exhibited that **8a–h** displayed dramati-

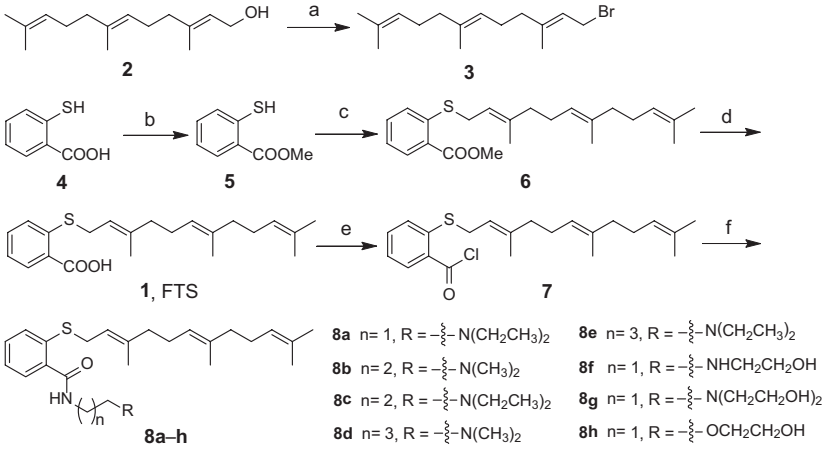

Scheme 1. Reaction conditions and reagents: (a) PBr_3, *n*-hexane, pyridine, ether, 0°C to rt, 4 h, 76%; (b) $SOCl_2$, MeOH, 0°C–reflux, 8 h, 85%; (c) **3**, K_2CO_3, CH_3CN, 50°C, 6 h, 82%; (d) 1 N NaOH, MeOH, 60°C, 10 h, 90%; (e) oxalylchloride, CH_2Cl_2, rt, 4 h; and (f) different substituted diamines, TEA, CH_2Cl_2, −10°C to rt, 2 h.

Table 1. The IC_{50} values of **8a–h** against seven human cancer cell lines.

Compd.	*In vitro* inhibition of human cancer cell proliferation (IC_{50},[a)] μM)						
	SMMC-7721	Panc-1	EJ	SGC-7901	SKOV-3	H460	MCF-7
FTS	69.7	53.6	47.6	41.3	51.2	49.2	49.1
Sorafenib	18.7	12.3	22.9	11.5	9.25	10.8	9.12
8a	26.3	23.6	28.5	21.1	23.4	27.8	22.3
8b	9.45	14.3	11.6	16.4	17.7	15.5	19.0
8c	8.22	12.5	7.52	7.36	8.05	12.8	13.9
8d	8.72	9.32	10.3	8.92	13.4	10.6	11.3
8e	7.15	7.85	8.31	8.03	9.45	7.43	8.98
8f	6.20	6.25	6.77	7.67	6.63	7.83	7.55
8g	6.55	7.29	7.70	7.91	9.02	8.05	9.26
8h	11.8	15.7	12.5	12.3	17.9	14.9	16.4

[a)] The inhibitory effects of individual compounds on the proliferation of cancer cell lines were determined by the MTT assay and expressed as the IC_{50} (the dose achieving 50% inhibition in the proliferation of cancer cells cultured).

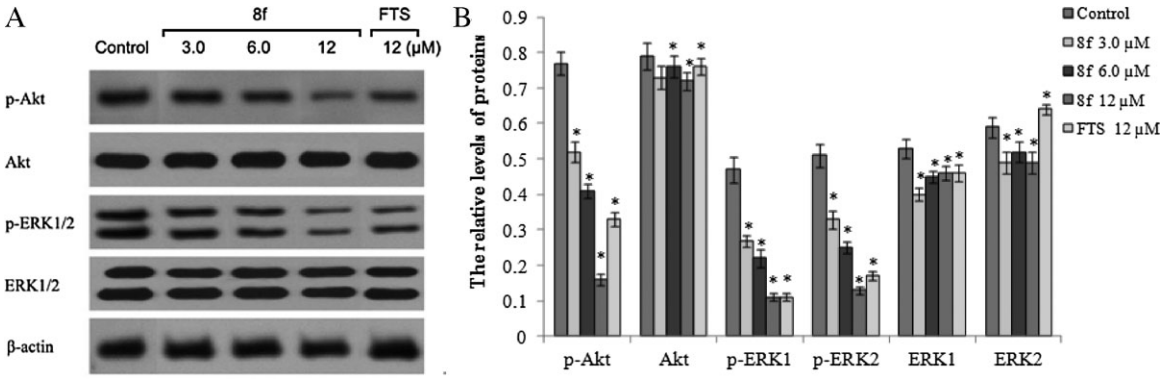

Figure 1. Immunoblot analysis of the expression and phosphorylation of Akt, and ERK1/2 *in vitro*. (A) SMMC-7721 cells treated with vehicle (control), FTS, or different doses of **8f** were homogenized, and their lysates were subjected to immunoblot analysis using anti-Akt, antiphospho-Akt (Ser473), anti-ERK, antiphospho-ERK (Thr202/Tyr204), and anti-β-actin antibodies, respectively. (B) Quantitative analysis. The relative levels of each signaling event to control β-actin were determined by densimetric scanning. The data are expressed as means ± SEM of three duplicate experiments. $^{*}P < 0.01$ versus control.

cally improvement in antitumor activities with the IC_{50} values to reach a low micromolar range compared to FTS and suggesteded that SMMC-7721 cells were more sensetive to the tested compounds (except **8a**). Moreover, the inhibitory effects of **8e–g** ($IC_{50} = 6.20–9.45\ \mu M$ range) on the proliferation of each tested human cancer cell line were slightly stronger than that of sorafenib ($IC_{50} = 9.12–22.9\ \mu M$), much higher than that of FTS ($IC_{50} = 41.3–69.7\ \mu M$). Notably, among them, compound **8f** showed the strongest antitumor activities with IC_{50} values of 6.20–7.83 μM, which was one- to threefold less than those of sorafenib and six- to tenfold less than that of FTS *in vitro* and **8f** was selected for further biological evaluation.

To determine whether the inhibitory activities of these FTS derivatives were associated with Ras-related signaling pathway, the effect of **8f** on the Ras-related signaling in SMMC-7721 cells (incubated with vehicle alone or with **8f** at 3, 6, or 12 μM and FTS at 12 μM) was determined by an immunoblotting assay. The expression and phosphorylation levels of the Ras-related signal events, Akt, and ERK (extracellular signal-regulated kinase) were determined (as shown in Fig. 1) using β-actin as the control. The levels of phospho-ERK1/2 and phospho-Akt were clear decreased in SMMC-7721 cells in a dose-dependent manner, while the expression of ERK1/2 and Akt showed remain the similar. The results suggested that the antitumor activities of **8f** may attribute to the inhibition of Ras-related signaling pathway.

As mentioned above, FTS and its derivatives could effectively block the Ras-related signaling pathway which was associated with activated apoptosis. To further examine the involvement of apoptosis in the antiproliferative effects of **8f**, apoptosis assay employing SMMC-7721 cells was assessed. The SMMC-7721 cells were incubated with vehicle alone (0.1% DMSO) or with **8f** at 3, 6, or 12 μM and 12 μM of FTS for 48 h, and stained with FITC-Annexin V and propidium iodide (PI). The percentages of apoptotic cells were determined by flow cytometry analysis. The effect of **8f** on cell apoptosis is depicted in Fig. 2A. It showed that the SMMC-7721 cell apoptosis rate was unobvious in the untreated group. However, in **8f**-treated SMMC-7721 cell, the frequency of the cell apoptosis showed an upward trend with the dose increased. As shown in Fig. 2B, low concentration (3 μM) of **8f** only induced 16.7% apoptosis activity on SMMC-7721 cells. And following treatment with 12 μM of **8f** induced 83.3% of SMMC-7721 cell apoptosis, which was significantly higher frequency of the cell apoptosis than that of FTS with the same concentration. The observations revealed that the antitumor activity of **8f** appeared to be concentration-dependent and the apoptosis effect of **8f** was significantly improved compared to the parent compound FTS.

Structure–activity relationships (SARs)

Analysis of SAR revealed that antitumor activities of farnesylthiosalicylamides **8a–h** were improved after FTS connecting with different substituted diamines, and were comparable to or slightly weaker than previously published farnesylthiosalicylamides [20, 21]. The evaluations suggested that the improvement of the antitumor activities may attribute to be the exposed basic functionalities of terminal substituted amines in farnesylthiosalicylamide derivatives **8a–g**, which could improve aqueous solubility thereby leading to the more facilitative to penetrate the cancer cells and reduce the metabolism of the active molecules. For example, compound **8f** or **8g** with basic functionalities of ethanolamine exhibited more potent antiproliferative activities than compound **8h** with non-basic functionalities of hydroxyethyl ether group. In addition, refer to **8a–e**,

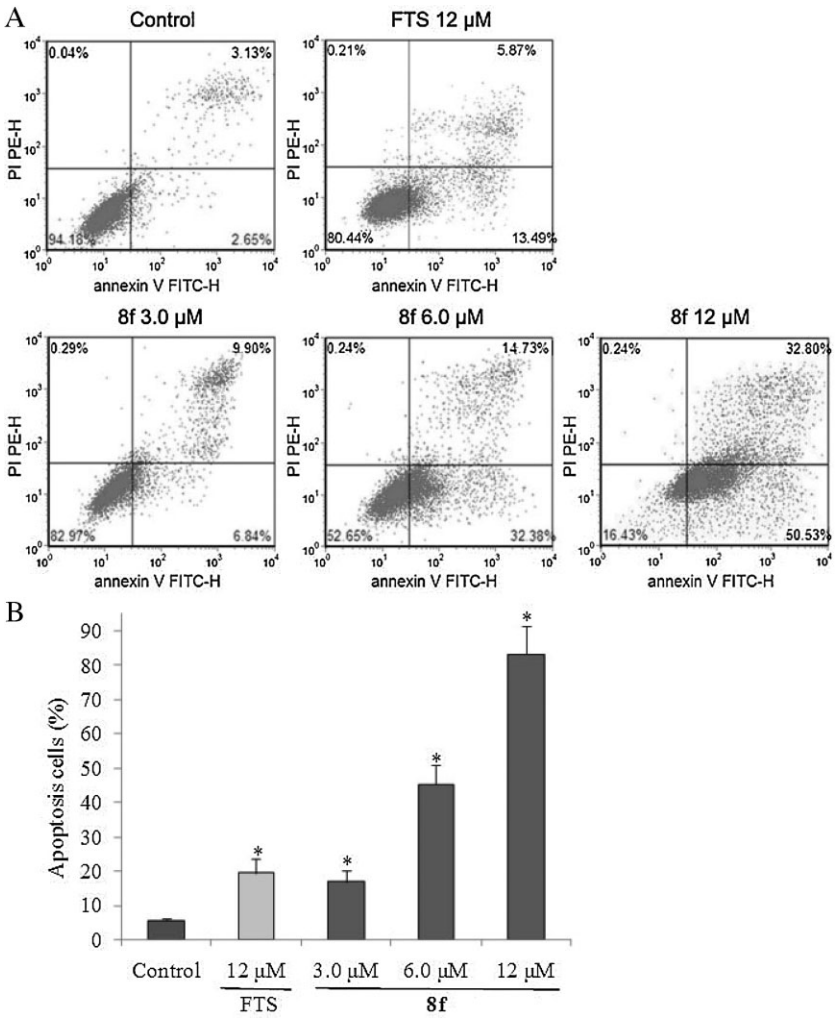

Figure 2. Compound **8f** induced SMMC-7721 cell apoptosis *in vitro*. SMMC-7721 cells were incubated with the indicated concentrations of **8f** and 12 μM FTS for 48 h, and the cells were stained with FITC-Annexin V and PI, followed by flow cytometry analysis. (A) Flow cytometry analysis. (B) Quantitative analysis of apoptotic cells. Data are expressed as means ± SEM of the percentages of apoptotic cells from three independent experiments. $^{*}P < 0.01$ versus control.

compounds with longer chain length, showed relatively stronger antitumor activities. Furthermore, compound **8f** displayed the most potent against tumor cells. One plausible explanation is that **8f** with more hydrogen bonds may be more active to bind the galectin site of farnesyl-Ras, thus displaying stronger antitumor activities. On the contrary, with the replacing of the *N*-atom of terminal tertiary amine with an oxygen atom, biological activities of **8h** were reduced. However, further investigation about the precise SAR of these compounds is ongoing.

Conclusions

In summary, we synthesized a series of FTS derivatives which were conjugated FTS with different substituted diamines. The *in vitro* assay of their inhibitory activities against seven tumor cell lines showed that farnesylthiosalicylamide derivatives displayed strong antitumor activities. Especially, compound **8f** had a good potency superior to FTS and sorafenib, which was probably responsible for the appropriate chain length as well as the better solubility of diamines. Furthermore, treatment with **8f** could lead to effective inhibition of the Ras-related signaling pathway in a dose-dependent manner in cancer cells. More importantly, compound **8f** could induce tumor cell apoptosis more potently than FTS. The further investigation is ongoing for more precise SAR and more potent agents.

Experimental

Chemistry

Infrared (IR) spectra (KBr) were recorded on a Nicolet Impact 410 instrument (KBr pellet). ^{1}H NMR spectra were recorded with a Bruker Avance 300 MHz spectrometer at 300 K, using TMS as an

internal standard. MS spectra were recorded on a Mariner Mass Spectrum (ESI). Element analysis was performed on an Eager 300 instrument. All compounds were routinely checked by TLC and ^{1}H NMR. TLCs and preparative thin-layer chromatography were performed on silica gel GF/UV 254, and the chromatograms were conducted on silica gel (200–300 mesh, Merck) and visualized under UV light at 254 and 365 nm. All solvents were reagent grade and, when necessary, were purified and dried by standard methods. Solutions after reactions and extractions were concentrated using a rotary evaporator operating at a reduced pressure of ca. 20 Torr. Organic solutions were dried over anhydrous sodium sulfate.

(2E,6E)-1-Bromo-3,7,11-trimethyldodeca-2,6,10-triene ***3***

To a solution of farnesol **2** (2.87 g, 12.9 mmol) in diethyl ether (15 mL) and pyridine (0.1 mL) under nitrogen atmosphere, PBr_3 (1.52 g, 5.6 mmol) dissolved with *n*-hexane (6 mL) was added at 0°C, and then the mixture was stirred for 0.5 h and following for 2 h at room temperature. The upper layer was poured into ice water, and extracted with diethyl ether (20 mL × 3). The organic layer was combined, washed with brine, dried over anhydrous Na_2SO_4, and concentrated *in vacuo* to afford **3** as a colorless liquid (2.79 g, 76%).

Methyl 2-mercaptobenzoate ***5***

To a methanol solution (50 mL) of thiosalicylic acid **4** (5 g, 32.5 mmol), $SOCl_2$ was added slowly and the mixture was stirred for 1 h at 0°C, then warmed up to the room temperature and refluxed for 6 h. The solvent was evaporated under reduced pressure. The residue was dissolved in ethyl acetate (50 mL), and then the solution was washed with saturated $NaHCO_3$ (50 mL × 2) and brine, dried with anhydrous Na_2SO_4. The crude product was purified by silica gel chromatography (petroleum ether–ethyl acetate = 40:1 v/v as the eluent) to afford compound **5** as a colorless liquid (4.62 g, 85%).

Methyl 2-(((2E,6E)-3,7,11-trimethyldodeca-2,6,10-trien-1-yl)thio)benzoate ***6***

A mixture of **5** (1.8 g, 12 mmol), K_2CO_3 (2.6 g, 14 mmol), and **3** (3.4 g, 12 mmol) in acetonitrile (80 mL) was refluxed for 6 h. The solvent was evaporated in vacuum and water was added. The solution was neutralized with 2 N HCl solution to pH 6–7, and then extracted with CH_2Cl_2 (20 mL × 3). The organic layer was concentrated *in vacuo* and the residue was purified by column chromatography on silica gel (petroleum ether–ethyl acetate = 30:1 v/v as the eluent), yield **6** as yellowish oil (3.66 g, 82%). ^{1}H NMR ($CDCl_3$, 300 MHz, δ ppm): 7.96 (m, 1H, Ar-H), 7.74 (m, 1H, Ar-H), 7.30 (m, 1H, Ar-H), 7.14 (m, 1H, Ar-H), 5.34 (m, 1H, $SCH_2C\underline{H}$), 5.09 (m, 2H, $2 \times CH_2C\underline{H}{=}CCH_3$), 3.92 (s, 3H, OCH_3), 3.58 (d, 2H, $J = 7.8$ Hz, $SC\underline{H}_2$), 1.89–2.02 (m, 8H, $2 \times CC\underline{H}_2C\underline{H}_2CH$), 1.50–1.68 (m, 12H, $4 \times CH{=}CC\underline{H}_3$).

2-(((2E,6E)-3,7,11-Trimethyldodeca-2,6,10-trien-1-yl)thio)-benzoic acid ***1***

Compound **6** (2.50 g, 6.72 mmol) was dissolved in 60 mL of methanol, then 1 N NaOH (10 mL) was added at room temperature. The mixture was stirred for 10 h at 60°C, and then cooled. The solvent was evaporated and the residue was dissolved in 1 M HCl solution and following extracted with ethyl acetate (30 mL × 3). The organic layer was combined, washed with brine, dried with anhydrous Na_2SO_4, and concentrated *in vacuo*, affording **1** as a pale yellow waxy solid (2.16 g, 90%). ^{1}H NMR ($CDCl_3$, 300 MHz, δ ppm): 8.15 (m, H, Ar-H), 7.47 (m, 1H, Ar-H), 7.42 (m, 1H, Ar-H), 7.26 (m, 1H, Ar-H), 5.31 (m, 1H, $SCH_2C\underline{H}$), 5.09 (m, 2H, $2 \times CH_2C\underline{H}{=}CCH_3$), 3.57 (d, 2H, $J = 4.5$Hz, SCH_2), 1.89–2.02 (m, 8H, $2 \times CC\underline{H}_2C\underline{H}_2CH$), 1.50–1.68 (m, 12H, $4 \times CH{=}CC\underline{H}_3$); MS (ESI) $m/z = 357$ $[M-1]^+$; Anal. calcd. for $C_{22}H_{30}O_2S$: C, 73.70; H, 8.43. Found: C, 73.77; H, 8.84.

2-(((2E,6E)-3,7,11-Trimethyldodeca-2,6,10-trien-1-yl)thio)-benzoyl chloride ***7***

The parent compound **1** (0.36 g, 1 mmol) was dissolved in anhydrous CH_2Cl_2 (6 mL), then oxalyl chloride (4 mmol) was dropwise added. The mixture was stirred for 4 h at room temperature. The solvent and excess oxalyl chloride was evaporated *in vacuo* to obtain the farnesylthiosalicyl chloride **7** with no need for further purification.

General procedure for the preparation of ***8a–h***

To a mixture of different substituted diamines (0.33 mmol) and TEA (0.45 mmol) in CH_2Cl_2 (10 mL) was dropwise added a CH_2Cl_2 solution (5 mL) of farnesylthiosalicyl chloride **7** (1.12 g, 0.3 mmol) at 0°C. After stirred for another 0.5 h the mixture was added 20 mL water and extracted with CH_2Cl_2 (20 mL × 3). The organic layer was combined, washed with brine, dried with anhydrous Na_2SO_4 and concentrated *in vacuo*. The crude product was separated by silica gel chromatography (CH_2Cl_2–MeOH = 4:1 as the eluent) to afford **8a–h** as a yellowish oil.

N-(2-(Diethylamino)ethyl)-2-(((2E,6E)-3,7,11-trimethyldodeca-2,6,10-trien-1-yl)thio)benzamide ***8a***

Yellowish oil, 78% yield. IR (KBr, cm^{-1}): 3420, 3156, 1690, 1605, 1593, 1420; ^{1}H NMR (DMSO-d_6, 300 MHz, δ ppm): 8.05 (m, 1H, Ar-H), 7.83 (m, 1H, Ar-H), 7.30–7.38 (m, 2H, Ar-H), 5.23 (m, 1H, $SCH_2C\underline{H}$), 5.07–5.09 (m, 2H, $2 \times CH_2C\underline{H}{=}CCH_3$), 3.56 (d, 2H, $J = 9.0$ Hz, SCH_2), 2.99–3.05 (m, 8H, $4 \times NCH_2$), 1.99 (m, 8H, $2 \times CC\underline{H}_2C\underline{H}_2CH$), 1.53–1.68 (m, 12H, $4 \times CH_3$), 0.98 (m, 6H, $2 \times CH_2C\underline{H}_3$); MS (ESI) $m/z = 457$ $[M+H]^+$; Anal. calcd. for $C_{28}H_{44}N_2OS$: C, 73.63; H, 9.71; N, 6.13. Found: C, 73.52; H, 9.94; N, 6.01.

N-(3-(Dimethylamino)propyl)-2-(((2E,6E)-3,7,11-trimethyldodeca-2,6,10-trien-1-yl)thio)benzamide ***8b***

Yellowish oil, 80% yield. IR (KBr, cm^{-1}): 3400, 3046, 1701, 1610, 1590, 1435; ^{1}H NMR (DMSO-d_6, 300 MHz, δ ppm): 7.98 (m, 2H, Ar-H), 7.31 (m, 2H, Ar-H), 5.33 (m, 1H, $SCH_2C\underline{H}$), 5.14 (m, 2H, $2 \times CH_2C\underline{H}{=}CCH_3$), 3.38 (d, 2H, $J = 9.0$ Hz, SCH_2), 3.05 (m, 2H, NCH_2), 2.47 (m, 2H, NCH_2), 2.24 (s, 6H, CH_3NCH_3), 1.90–1.99 (m, 8H, $2 \times CC\underline{H}_2C\underline{H}_2CH$), 1.54–1.69 (m, 14H, $4 \times CH_3$, $CH_2C\underline{H}_2CH_2$); MS (ESI) $m/z = 443$ $[M+H]^+$; Anal. calcd. for $C_{27}H_{42}N_2OS$: C, 73.25; H, 9.56; N, 6.33. Found: C, 73.42; H, 9.31; N, 6.25.

N-(3-(Diethylamino)propyl)-2-(((2E,6E)-3,7,11-trimethyldodeca-2,6,10-trien-1-yl)thio)benzamide ***8c***

Yellowish oil, 74% yield. IR (KBr, cm^{-1}): 3346, 3058, 1692, 1613, 1580, 1450; ^{1}H NMR (DMSO-d_6, 300 MHz, δ ppm): 8.08 (m, 1H, Ar-H), 7.89 (m, 1H, Ar-H), 7.30 (m, 2H, Ar-H), 5.23 (m, 1H, $SCH_2C\underline{H}$), 5.06 (m, 2H, $2 \times CH_2C\underline{H}{=}CCH_3$), 3.48–3.42 (m, 4H, SCH_2, NCH_2), 2.42 (m, 6H, $3 \times NCH_2$), 1.90–1.99 (m, 8H, $2 \times CC\underline{H}_2C\underline{H}_2CH$), 1.54–

1.69 (m, 14H, 4 × CH_3, $CH_2C\underline{H}_2CH_2$), 0.90 (m, 6H, 2 × $CH_2C\underline{H}_3$); MS (ESI) $m/z = 471$ $[M+H]^+$; Anal. calcd. for $C_{29}H_{46}N_2OS$: C, 73.99; H, 9.85; N, 5.95. Found: C, 74.21; H, 9.47; N, 6.09.

N-(4-(Dimethylamino)butyl)-2-(((2E,6E)-3,7,11-trimethyldodeca-2,6,10-trien-1-yl)thio)benzamide ***8d***

Yellowish oil, 72% yield. IR (KBr, cm^{-1}): 3441, 3064, 1683, 1601, 1582, 1458; ^1H NMR (DMSO-d_6, 300 MHz, δ ppm): 8.04 (m, 1H, Ar-H), 7.76 (m, 1H, Ar-H), 7.30 (m, 2H, Ar-H), 5.24 (m, 1H, $SCH_2C\underline{H}$), 5.03 (m, 2H, 2 × $CH_2C\underline{H}$=CCH_3), 3.54–3.33 (m, 4H, SCH_2, NCH_2), 2.47 (m, 2H, CH_2N), 2.24 (s, 6H, 2 × NCH_3), 1.94–2.00 (m, 8H, 2 × $CC\underline{H}_2C\underline{H}_2CH$), 1.53–1.74 (m, 16H, 4 × CH=$CC\underline{H}_3$, $CH_2C\underline{H}_2C\underline{H}_2CH_2$); MS (ESI) $m/z = 457$ $[M+H]^+$; Anal. calcd. for $C_{28}H_{44}N_2OS$: C, 73.63; H, 9.71; N, 6.13. Found: C, 73.52; H, 9.90; N, 6.28.

N-(4-(Diethylamino)butyl)-2-(((2E,6E)-3,7,11-trimethyldodeca-2,6,10-trien-1-yl)thio)benzamide ***8e***

Yellowish oil, 76% yield. IR (KBr, cm^{-1}): 3380, 3114, 1704, 1615, 1578, 1460; ^1H NMR (DMSO-d_6, 300 MHz, δ ppm): 7.99 (m, 2H, Ar-H), 7.27 (m, 2H, Ar-H), 5.32 (m, 1H, $SCH_2C\underline{H}$), 5.03 (m, 2H, 2 × $CH_2C\underline{H}$=CCH_3), 3.55 (d, 2H, $J = 9.0$ Hz, SCH_2), 3.32 (m, 2H, $NHC\underline{H}_2$), 2.42 (m, 6H, 3 × CH_2N), 1.90–2.02 (m, 8H, 2 × $CC\underline{H}_2C\underline{H}_2CH$), 1.54–1.76 (m, 16H, 4 × CH=$CC\underline{H}_3$, $CH_2C\underline{H}_2C\underline{H}_2CH_2$), 0.93 (m, 6H, 2 × $CH_2C\underline{H}_3$); MS (ESI) $m/z = 485$ $[M+H]^+$; Anal. calcd. for $C_{30}H_{48}N_2OS$: C, 74.33; H, 9.98; N, 5.78. Found: C, 74.59; H, 9.76; N, 5.93.

N-(2-((2-Hydroxyethyl)amino)ethyl)-2-(((2E,6E)-3,7,11-trimethyldodeca-2,6,10-trien-1-yl)thio)benzamide ***8f***

Yellowish oil, 68% yield. IR (KBr, cm^{-1}): 3360, 3081, 1688, 1616, 1585, 1448; ^1H NMR (DMSO-d_6, 300 MHz, δ ppm): 8.18 (m, 1H, Ar-H), 7.34–7.41 (m, 3H, Ar-H), 7.22 (m, 1H, Ar-H), 5.23 (m, 1H, $SCH_2C\underline{H}$), 5.06–5.08 (m, 2H, 2 × $CH_2C\underline{H}$=CCH_3), 3.10–3.60 (m, 6H, SCH_2, $CONHC\underline{H}_2$, CH_2O), 2.49–2.69 (m, 4H, $C\underline{H}_2NHC\underline{H}_2$), 1.99 (m, 8H, 2 × $CC\underline{H}_2C\underline{H}_2CH$), 1.60–1.68 (m, 12H, 4 × CH_3); MS (ESI) $m/z = 445$ $[M+1]^+$; Anal. calcd. for $C_{26}H_{40}N_2O_2S$: C, 70.23; H, 9.07; N, 6.30. Found: C, 70.34; H, 8.96; N, 6.35.

N-(2-(Bis(2-hydroxyethyl)amino)ethyl)-2-(((2E,6E)-3,7,11-trimethyldodeca-2,6,10-trien-1-yl)thio)benzamide ***8g***

Yellowish oil, 52% yield. IR (KBr, cm^{-1}): 3385, 1895, 1602, 1580, 1466; ^1H NMR (DMSO-d_6, 300 MHz, δ ppm): 7.91 (m, 1H, Ar-H), 7.50 (m, 1H, Ar-H), 7.35 (m, 2H, Ar-H), 5.41 (m, 1H, $SCH_2C\underline{H}$), 5.12 (m, 2H, 2 × $CH_2C\underline{H}$=CCH_3), 3.66 (m, 2H, 2 × OH), 3.51–3.30 (m, 8H, SCH_2, $CONCH_2$, 2 × $C\underline{H}_2OH$), 2.69–2.53 (m, 6H, 3 × NCH_2), 1.92–2.01 (m, 8H, 2 × $CC\underline{H}_2C\underline{H}_2CH$), 1.52–1.77 (m, 14H, 4 × CH_3, $CH_2C\underline{H}_2CH_2$); MS (ESI) $m/z = 489$ $[M+1]^+$; Anal. calcd. for $C_{28}H_{44}N_2O_3S$: C, 68.81; H, 9.07; N, 5.73. Found: C, 68.57; H, 9.23; N, 5.56.

N-(2-(2-Hydroxyethoxy)ethyl)-2-(((2E,6E)-3,7,11-trimethyldodeca-2,6,10-trien-1-yl)thio)benzamide ***8h***

Yellowish oil, 65% yield. IR (KBr, cm^{-1}): 3356, 3133, 1696, 1606, 1578, 1455; ^1H NMR (DMSO-d_6, 300 MHz, δ ppm): 8.03 (m, 1H, Ar-H), 7.46 (m, 1H, Ar-H), 7.32 (m, 2H, Ar-H), 5.25 (m, 1H, $SCH_2C\underline{H}$), 5.07–5.09 (m, 2H, 2 × $CH_2C\underline{H}$=CCH_3), 3.47–3.72 (m, 10H, SCH_2, $NHC\underline{H}_2C\underline{H}_2O$, $OC\underline{H}_2C\underline{H}_2OH$), 1.99 (m, 8H, 2 × $CC\underline{H}_2C\underline{H}_2CH$), 1.57–1.73 (m, 12H, 4 × CH_3); MS (ESI) $m/z = 446$ $[M+1]^+$; Anal. calcd. for $C_{26}H_{39}N_2O_3S$: C, C, 70.07; H, 8.82; N, 3.14. Found: C, 70.23; H, 8.58; N, 3.25.

Biological activity

MTT assay

SMMC-7721 (human hepatocellular carcinoma cells), Panc-1 (human pancreatic carcinoma cells), EJ (human bladder carcinoma cells), SGC7901 (human gastric cancer cells), SKOV-3 (human ovarian cancer cells), H460 (human lung cancer cells), and MCF-7 (human breast cancer cells) at 10^4 cells per well were cultured in 100 μL 10% FBS DMEM in 96-well flat-bottom microplates overnight. The cells were incubated in triplicate with 0.1% DMSO or different concentrations (1.5, 3.0, 6.0, 12, 25, or 50 μM) of each test compound for 48 h. During the last 4 h incubation, 30 μL of tetrazolium dye (MTT) solution (5 mg/mL) was added to each well. The resulting MTT-formazan crystals were dissolved in 150 μL DMSO, and absorbance was measured spectrophotometrically at 570 nm using an ELISA plate reader. The inhibition induced by each test compound at the indicated concentrations was expressed as a percentage. The concentration required for 50% inhibition (IC_{50}) was calculated using the software (GraphPadPrism Version 4.03).

Western blot assay

The mechanisms of the inhibitory activity of Ras-related signaling were determined by Western blot assay. SMMC-7721 cells at 1.5×10^5/mL were treated with 3.0, 6.0, or 12 μM **8f** or vehicle control (0.1% of DMSO) in 2 mL DMEM medium supplemented with 10% FBS for 8 h. After harvesting and lysis, the cell lysates (50 μg/lane) were separated by SDS–PAGE (12% gel) and transferred onto nitrocellulose membranes. After blocking with 5% fat-free milk, the target proteins were probed with anti-Akt, anti-phospho-Akt (Ser473), anti-ERK, anti-phospho-ERK (Thr202/Tyr204), and anti-β-actin antibodies (Cell Signaling, Boston), respectively. The bound antibodies were detected by HRP-conjugated second antibodies and visualized using the enhanced chemiluminescent reagent. The relative levels of each signaling event to control β-actin were determined by densimetric scanning.

Flow cytometry assay of cell apoptosis

SMMC-7721 (5×10^5) cells were seeded into 6-well plates for 24 h, and incubated in triplicate with the test compound (3.0, 6.0, and 12 μM) or vehicle (0.1% of DMSO) in 2 mL DMEM medium supplemented with 10% FBS for 48 h. The cells were harvested, and stained with FITC-Annexin V and PI (BioVision) at room temperature for 15 min. The percentage of apoptotic cells was determined by flow cytometry (Beckman Coulter) analysis.

Statistical analysis

All data were expressed as means ± SEM. Statistical differences between groups were analyzed by one-way analysis of variance with subsequent Tukey's tests. In all cases, $P < 0.05$ was considered statistically significant.

We gratefully acknowledge the financial support by the Natural Science Foundation of China (Grant Nos. 81302628 and 81202467) and Jiangsu Province (Grant Nos. BK2011389 and BK2012232), the Natural Science Research Project of Universities in Jiangsu Province of China (11KJB350004), Applied Research Projects of Nantong City (BK2012085), and also thank a project funded by the Priority Academic Programs Development of Jiangsu Higher Education Institutions (PAPD).

The authors have declared no conflict of interest.

References

[1] J. L. Bos, *Cancer Res.* **1989**, *49*, 4682–4689.

[2] A. D. Cox, C. J. Der, *Oncogene* **2003**, *22*, 8999–9006.

[3] S. Schubbert, K. Shannon, G. Bollag, *Nat. Rev. Cancer* **2007**, *7*, 295–308.

[4] D. Bar-Sagi, A. Hall, *Cell* **2000**, *103*, 227–238.

[5] M. E. Pacold, S. Suire, O. Perisic, S. Lara-Gonzalez, C. T. Davis, E. H. Walker, P. T. Hawkins, L. Stephens, J. F. Eccleston, R. L. Williams, *Cell* **2000**, *103*, 931–943.

[6] E. Porfiri, F. McCormick, *J. Biol. Chem.* **1996**, *271*, 5871–5877.

[7] A. A. Adjei, *J. Natl. Cancer Inst.* **2001**, *93*, 1062–1074.

[8] T. Yokota, *Anticancer Agents Med. Chem.* **2012**, *12*, 163–171.

[9] L. Chin, A. Tam, J. Pomerantz, M. Wong, J. Holash, N. Bardeesy, Q. Shen, R. O'Hagan, J. Pantginis, H. Zhou, J. W. Horner, C. Cordon-Cardo, G. D. Yancopoulos, R. A. DePinho, *Nature* **1999**, *400*, 468–472.

[10] R. Haklai, M. G. Weisz, G. Elad, A. Paz, D. Marciano, Y. Egozi, G. Ben-Baruch, Y. Kloog, *Biochemistry* **1998**, *37*, 1306–1314.

[11] M. Marom, R. Haklai, G. Ben-Baruch, D. Marciano, Y. Egozi, Y. Kloog, *J. Biol. Chem.* **1995**, *270*, 22263–22270.

[12] A. M. Tsimberidou, M. A. Rudek, D. Hong, C. S. Ng, J. Blair, H. Goldsweig, R. Kurzrock, *Cancer Chemother. Pharmacol.* **2010**, *65*, 235–241.

[13] N. Charette, C. D. Saeger, Y. Horsmans, I. Leclercq, P. St rke, *Cell Death Dis.* **2013**, *4*, e471.

[14] N. Charette, C. D. Saeger, V. Lannoy, Y. Horsmans, I. Leclercq, P. Stärkel, *Mol. Cancer* **2010**, *9*, 256.

[15] D. Laheru, P. Shah, N. V. Rajeshkumar, F. McAllister, G. Taylor, H. Goldsweig, D. T. Le, R. Donehower, A. Jimeno, S. Linden, M. Zhao, D. Song, M. A. Rudek, M. Hidalgo, *Invest. New Drugs* **2012**, *30*, 2391–2399.

[16] G. J. Riely, M. L. Johnson, C. Medina, N. A. Rizvi, V. A. Miller, *J. Thorac. Oncol.* **2011**, *6*, 1435–1437.

[17] E. Bustinza-Linares, R. Kurzrock, A.-M. Tsimberidou, *Future Oncol.* **2010**, *6*, 885–891.

[18] D. J. St. Jean, Jr., C. Fotsch, *J. Med. Chem.* **2012**, *55*, 6002–6020.

[19] S. Cogoi, A. E. Shchekotikhin, A. Membrino, Y. B. Sinkevich, L. E. Xodo, *J. Med. Chem.* **2013**, *56*, 2764–2778.

[20] L. Goldberg, R. Haklai, V. Bauer, A. Heiss, Y. Kloog, *J. Med. Chem.* **2009**, *52*, 197–205.

[21] Y. Ling, X. L. Ye, Z. Z. Zhang, Y. H. Zhang, Y. S. Lai, H. Ji, S. X. Peng, J. D. Tian, *J. Med. Chem.* **2011**, *54*, 3251–3259.

